Molecular Microbiology (2013) 87(3), 672–689 ■
doi:10.1111/mmi.12125
First published online 26 December 2012

The group A streptococcal collagen-like protein-1, Scl1, mediates biofilm formation by targeting the extra domain A-containing variant of cellular fibronectin expressed in wounded tissue

Heaven Oliver-Kozup,[1] Karen H. Martin,[2,3] Diane Schwegler-Berry,[4] Brett J. Green,[5] Courtney Betts,[6†] Arti V. Shinde,[6‡] Livingston Van De Water[6] and Slawomir Lukomski[1]*

[1]*Department of Microbiology, Immunology, and Cell Biology, West Virginia University School of Medicine, Morgantown, WV 26506, USA.*
[2]*Mary Babb Randolph Cancer Center, West Virginia University School of Medicine, Morgantown, WV 26506, USA.*
[3]*Microscope Imaging Facility, West Virginia University School of Medicine, Morgantown, WV 26506, USA.*
[4]*Pathology and Physiology Research Branch, Health Effects Laboratory Division, National Institute of Occupational Safety and Health (NIOSH), Centers for Disease Control and Prevention, Morgantown, WV 26505, USA.*
[5]*Allergy and Clinical Immunology Branch, Health Effects Laboratory Division, National Institute of Occupational Safety and Health (NIOSH), Centers for Disease Control and Prevention, Morgantown, WV 26505, USA.*
[6]*Center for Cell Biology and Cancer Research, Albany Medical College, Albany, NY 12208, USA.*

Summary

Wounds are known to serve as portals of entry for group A *Streptococcus* (GAS). Subsequent tissue colonization is mediated by interactions between GAS surface proteins and host extracellular matrix components. We recently reported that the streptococcal collagen-like protein-1, Scl1, selectively binds the cellular form of fibronectin (cFn) and also contributes to GAS biofilm formation on abiotic surfaces. One structural feature of cFn, which is predominantly expressed in response to tissue injury, is the presence of a spliced variant containing extra domain A (EDA/EIIIA). We now report that GAS biofilm formation is mediated by the Scl1 interaction with EDA-containing cFn. Recombinant Scl1 proteins that bound cFn also bound recombinant EDA within the C-C' loop region recognized by the $\alpha_9\beta_1$ integrin. The extracellular 2-D matrix derived from human dermal fibroblasts supports GAS adherence and biofilm formation. Altogether, this work identifies and characterizes a novel molecular mechanism by which GAS utilizes Scl1 to specifically target an extracellular matrix component that is predominantly expressed at the site of injury in order to secure host tissue colonization.

Accepted 4 December, 2012. *For correspondence. E-mail slukomski@hsc.wvu.edu; Tel. (+1) 304 293 6405; Fax (+1) 304 293 7328. Current addresses: †Department of Cell Biology, Stem Cells, and Development, University of Colorado Denver, Anschutz Medical Campus, Aurora, CO 80045, USA; ‡Department of Medicine-Cardiology, Albert Einstein College of Medicine, Bronx, NY 10461, USA.

Introduction

Group A *Streptococcus* (GAS) is responsible each year for more than 730 million infections worldwide ranging from the clinically uncomplicated (pharyngitis, impetigo) to severe and invasive diseases (necrotizing fasciitis, toxic shock), and autoimmune complications (Carapetis *et al.*, 2005; Tart *et al.*, 2007). GAS causes over 100 million skin infections and is categorized as transient or contaminant flora of the skin (Tognetti *et al.*, 2012). These infections are initiated via a portal of entry resulting from simple skin infringements, such as insect bites or cuts and scratches, as well as from more serious post-surgical wounds. For successful colonization within a wounded site, GAS utilizes surface adhesins to secure binding to host extracellular matrix (ECM) components (Chhatwal and Preissner, 2000), including collagen, fibronectin (Fn) and laminin.

The streptococcal collagen-like protein-1 (Scl1) is a ubiquitous surface adhesin, which is coexpressed with a range of known virulence factors that are regulated by the multiple virulence gene regulator of GAS (Mga) (Lukomski *et al.*, 2000a; 2001; Rasmussen *et al.*, 2000; Almengor *et al.*, 2006). Scl1 is a homotrimeric protein protruding from the GAS surface that contains four structurally distinct regions. The outermost N-terminal variable (V) region

is adjacent to a collagen-like (CL) region that consists of a varying number of GlyXaaYaa (GXY) repeats and adopts stable CL triple helices (Xu *et al*., 2002; Mohs *et al*., 2007). At the C-terminus, Scl1 contains a linker (L) region which is a series of conserved, direct repeats adjoining the CL region to the cell wall/membrane (WM)-associated region. Functionally, Scl1 was shown to bind to host-cell integrin receptors (Humtsoe *et al*., 2005; Caswell *et al*., 2007; 2008a) and plasma components (Han *et al*., 2006a; Påhlman *et al*., 2007; Gao *et al*., 2010). We recently reported that Scl1 selectively binds to cellular fibronectin (cFn), but not plasma fibronectin (pFn) (Caswell *et al*., 2010). Scl1 is also recognized to play a significant role in biofilm formation on abiotic surfaces (Oliver-Kozup *et al*., 2011).

The wound healing process is dependent on the interaction of cells with the surrounding ECM, which induces the formation of an ECM scaffold to promote cell migration and wound closure. A fundamental component within the ECM contributing to this process is cFn (Martin, 1997). The cFns form a large heterogeneous group of glycoproteins with isoforms resulting from alternative splicing events of pre-mRNA of a single gene (Pankov and Yamada, 2002). The soluble pFn is predominantly produced by hepatocytes, whereas cFn can be produced by diverse cell types and may generate up to 20 isoforms in humans. It contains varying amounts of two extra domains termed EDA (EIIIA) and EDB (EIIIB). EDA- and EDB-expressing cFn is highly regulated and plays a crucial role during embryogenesis and early development, and under non-diseased states is maintained at low levels within tissue of adult humans. The expression of cFn containing EDA (EDA/cFn) is upregulated during tissue repair and likely promotes wound cell function by the direct binding of $\alpha_4\beta_1$, $\alpha_4\beta_7$ and $\alpha_9\beta_1$ integrins (Ffrench-Constant *et al*., 1989; Sakai *et al*., 2001; Liao *et al*., 2002; Singh *et al*., 2004; Humphries *et al*., 2006; Kohan *et al*., 2010; To and Midwood, 2011).

In this work, we characterized the Scl1–cFn interaction using recombinant Scl proteins (rScl) derived from epidemiologically distinct GAS strains and investigated the significance of this binding during GAS biofilm formation. We report that Scl1 protein selectively targets the EDA domain of cFn, which is expressed during tissue repair. We mapped the Scl1 binding site within the C-C' loop region of EDA using peptide inhibition and antibody blocking assays, which overlaps with the EDA-$\alpha_9\beta_1$-integrin-binding site. Furthermore, the Scl1–ECM binding contributes significantly to GAS biofilm formation, which can be inhibited by either the treatment with the synthetic C-C' loop peptide or with the anti-EDA monoclonal antibody (mAb), IST-9. In conclusion, this work identifies a novel cFn-binding mechanism, which is conserved among pathogenically varying strains of GAS, and is mediated by Scl1 binding to the EDA/cFn variant that is expressed at the portal of pathogen entry. The Scl1–EDA/cFn binding may extend the time for GAS tissue colonization by impairing cFn–integrin binding and thereby delaying wound healing.

Results

The Scl1*–cFn interaction is mediated by the EDA domain of cFn*

In a previous study, we established that the Scl1 protein selectively binds the tissue ECM component, cFn (Fig. 1A) but not pFn (Caswell *et al*., 2010). Based on this finding, we hypothesized that the Scl1–cFn interaction is mediated via EDA, a domain that is not found in pFn, but is thought to be an integral component to the wound healing process. To test this hypothesis, we evaluated by direct ELISA the binding of ECM ligands to immobilized rScl1 proteins P176 (Scl1.41), P144 (Scl1.1) and P161 (Scl1.28) that were previously demonstrated to bind cFn (Caswell *et al*., 2010). An immobilized rScl2 construct, P163 (Scl2.28), served as a negative control for cFn binding. The ECM ligands (1 μg/well) tested included: (i) purified cFn as a positive control, and confirmed to contain the EDA/cFn variant using the EDA-specific mAb IST-9, (ii) the recombinant EDA (rEDA) and (iii) the recombinant type III domain four (rIII4), which differs by primary sequence but is structurally homologous to EDA and is common to both cFn and pFn. As shown in Fig. 1B, rScl1 proteins that are positive for cFn binding are also positive for binding to rEDA. In contrast, binding of the rIII4 to rScl1 proteins was comparable to that of the negative control, P163, for all three ECM ligands. When increasing concentrations (0.02–4.0 μM) of ECM ligands cFn, rEDA and rIII4 were incubated with immobilized rScl proteins to assess binding specificity, concentration-dependent binding of cFn and rEDA to all three rScl1 constructs was observed, plateauing around the 3–4 μM concentration (Fig. 1C). In contrast, no binding by rIII4 to rScl1 constructs was observed over the entire concentration range nor was binding by any ECM ligand to the negative control, P163, detected (data not shown). We also observed that rScl1 proteins bind better to cFn than rEDA construct. One possible explanation is that the EDA conformation in cFn and rEDA preparations is not identical or that rScl1 binding alters cFn structure (Mao and Schwarzbauer, 2005), resulting in improved binding. The latter mechanism would not be surprising as it has been reported for Fn binding by other bacterial adhesins, including streptococcal (M, F1/SfbI) and staphylococcal (FnbpA) proteins, as well as the BBK32 protein of *Borrelia burgdorferi* (House-Pompeo *et al*., 1996; Cue *et al*., 2001; Kim *et al*., 2004; Marjenberg *et al*., 2011). Altogether, our data indicate that the Scl1–cFn interaction is mediated, at least in part, via the EDA domain, and that this interaction is specific and concentration-dependent.

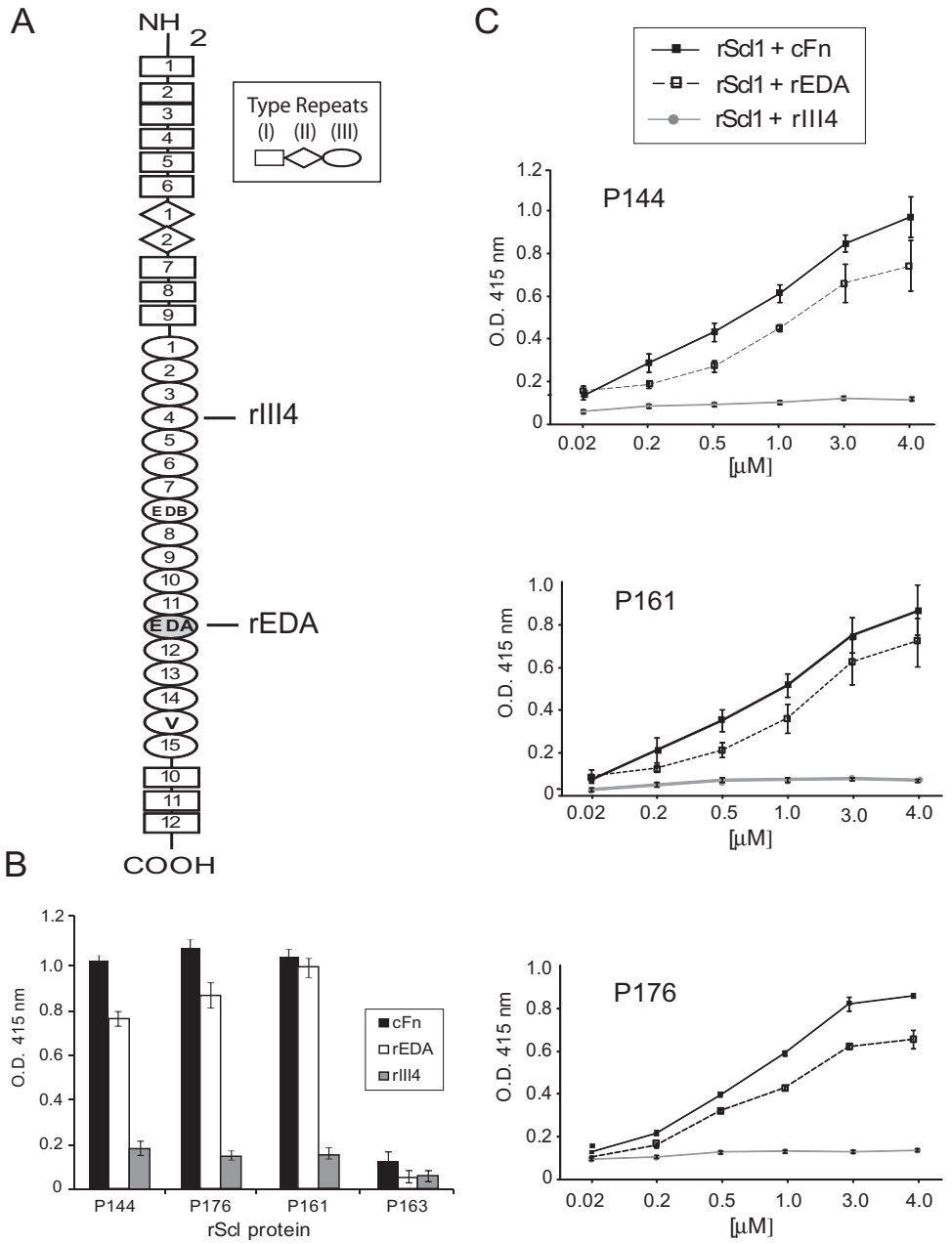

Fig. 1. The EDA domain mediates Scl1 binding to cFn.
A. Schematic representation of cFn. cFn monomer depicts type I, II and III repeats. The locations of the extra domain A (EDA) and type III repeat 4 are indicated, as sources for recombinant molecules rEDA and rIII4 used.
B. Binding of ECM ligands to recombinant Scl (rScl) proteins. cFn-binding positive recombinant Scl1 (rScl) proteins P144 (rScl1.1), P161 (rScl1.28) and P176 (rScl1.41), as well as cFn-binding negative control protein P163 (rScl2.28), were immobilized onto *Strep*-Tactin-coated wells and incubated with cFn or cFn-derived rEDA and rIII4 polypeptides. rScl-bound ligands were detected by ELISA with ligand-specific primary antibodies and appropriate HRP-conjugated secondary antibodies. Graphic bars indicate the mean $OD_{415\ nm}$ normalized against BSA controls. Statistical analysis was computed from three independent experimental repeats, each performed in triplicate wells ($n = 3 \pm$ SD).
C. Characterization of binding specificity between rScl proteins and ECM ligands. Immobilized rScl1 proteins, P144, P161 and P176, were incubated with increasing concentrations (0.02–4.0 μM) of cFn, rEDA and rIII4. Mean $OD_{415\ nm}$, $n = 3 \pm$ SD.

Mapping of Scl1 *binding site within EDA*

The cFn/EDA spliced variant produced in response to tissue injury (Ffrench-Constant *et al.*, 1989; Brown *et al.*, 1993; Serini *et al.*, 1998; Singh *et al.*, 2004) includes a loop region between the C and C' β-strands (Fig. 2A), which mediates binding to $\alpha_4\beta_1$ and $\alpha_9\beta_1$ integrins that actively participate in wound healing (Shinde *et al.*, 2008).

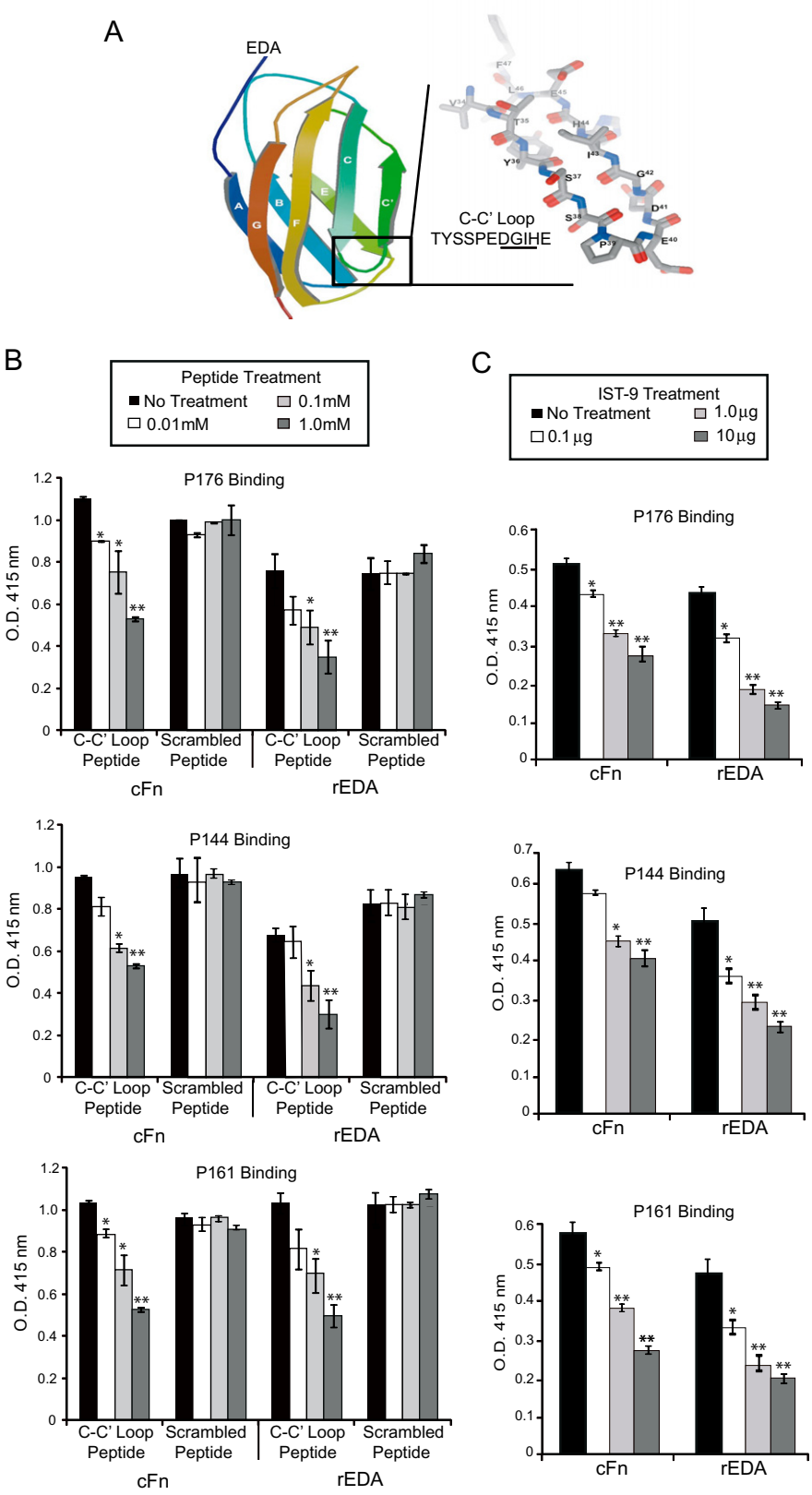

Fig. 2. Scl1–cFn interaction is mediated by the C-C' loop region of EDA. The Scl1 binding site within the EDA domain of cFn was mapped using peptide and antibody inhibition ELISAs. For both assays, recombinant cFn-binding positive proteins P144 (rScl1.1), P161 (rScl1.28) and P176 (rScl1.41) were immobilized onto *Strep*-Tactin-coated wells. Following incubation with peptide or mAb bound ECM ligands were detected with specific primary antibodies and the corresponding HRP-conjugated secondary antibodies. Graphic bars indicate the mean $OD_{415\ nm}$ normalized against BSA controls. Statistical analysis was computed from three independent experimental repeats, each performed in triplicate wells ($n = 3 \pm$ SD); $^{*}P \leq 0.05$, $^{**}P \leq 0.001$. Statistical significance evaluates differences in ligand binding between untreated and treated samples at the levels of $^{*}P \leq 0.05$, $^{**}P \leq 0.001$.
A. Structural representation of EDA. Ribbon model shows a β-sandwich composed of four β-strands, C, C', F and G, and the underlying three β-strands A, B and E (adapted from Shinde *et al.*, 2008). The stick representation of the C-C' loop is shown and its 11-amino-acid sequence is indicated. The adjacent key residues involved in $\alpha_9\beta_1$-integrin binding (D^{41} and G^{42}) and for the mAb IST-9 epitope (I^{43} and H^{44}) are underlined.
B. Peptide inhibition assay. Immobilized rScl1 proteins were pre-incubated with increasing concentrations (0.0–1.0 mM) of the synthetic C-C' loop peptide or the corresponding scrambled peptide, followed by the incubation with 0.25 µM ECM ligands, cFn and rEDA. ECM ligand binding to rScl1 is shown.
C. Antibody blocking assay. ECM ligands (0.25 µM) were pre-incubated with increasing concentrations (0.0–10 µg) of mAb IST-9. Mixtures were then added to rScl1-immobilized wells and allowed for rScl1–cFn/rEDA binding.

Fig. 3. Scl1–EDA interaction represents a common, cFn-binding mechanism among epidemiologically diverse GAS strains. Eleven rScl proteins derived from diverse GAS strains of various M types were tested for rEDA and cFn binding. rScl proteins tested included the cFn-binding positive rScl1 proteins P144 (rScl1.1), P161 (rScl1.28), P186 (rScl1.12), P190 (rScl1.2), P217 (rScl1.52) and P176 (rScl1.41), as well as cFn-binding negative rScl1 proteins P179 (rScl1.6) and P216 (rScl1.55), and rScl2 proteins P163 (rScl2.28), P177 (rScl2.4) and P178 (rScl2.77). rScl proteins were immobilized onto *Strep*-Tactin-coated wells and incubated with ECM ligands pFn, cFn and rEDA. rScl-bound ECM ligands were detected by ELISA with ligand-specific primary antibodies and the appropriate HRP-conjugated secondary antibodies. Graphic bars indicate the mean $OD_{415\,nm}$ normalized against BSA controls. Statistical analysis was computed from three independent experimental repeats, each performed in triplicate wells ($n = 3 \pm$ SD).
A. Identification of rScl1–ECM ligand binding. Immobilized rScl proteins were incubated with 1 μg per well of each ECM ligand. Designation of each rScl1 or rScl2 construct, as well as the GAS M type from which each construct was derived, is indicated.
B. Peptide inhibition assay. Immobilized rScl proteins were pre-incubated with a 1.0 mM concentration of the synthetic C-C' loop peptide or scrambled peptide and then with 1 μg of each cFn or rEDA ligand.
C. Antibody blocking assay. ECM ligands cFn and rEDA (1 μg) were pre-incubated with 10 μg per sample of mAb IST-9 and then added to rScl1-immobilized wells.

As loop regions are often involved in protein–protein interactions, we hypothesized that the C-C' loop region of EDA contains the Scl1 binding site. To test this, we examined the ability of an exogenous synthetic 11-amino-acid peptide (TYSSPEDGIHE), corresponding to the C-C' loop region of EDA, to inhibit binding of ECM ligands to immobilized rScl1 proteins, P176, P144 and P161. In this assay, increasing concentrations (0.01 mM, 0.1 mM and 1.0 mM) of the C-C' loop peptide or a scrambled peptide control (SEDIHYTEGPS) were pre-incubated with immobilized rScl proteins prior to the addition of the ECM ligands, cFn and rEDA. As shown in Fig. 2B, binding of cFn or rEDA to all three rScl1 proteins was inhibited by the C-C' loop peptide in a concentration-dependent manner up to 50% and 60% respectively, whereas no inhibition was observed with the scrambled peptide. These results mapped a Scl1 binding site to the EDA C-C' loop region.

Previous studies reported that residues Asp^{41} and Gly^{42} (Fig. 2A) within the C-C' loop region of EDA are involved in $\alpha_9\beta_1$-integrin binding and that the mAb IST-9 binds the C-C' loop of EDA at adjacent residues Ile^{43} and His^{44}, and blocks this integrin engagement (Liao *et al.*, 1999; Shinde *et al.*, 2008). We therefore used the anti-EDA mAb IST-9 to determine if Scl1 and $\alpha_9\beta_1$ integrin have overlapping binding sites within the EDA C-C' loop region (Fig. 2C). Both cFn and rEDA were pre-treated with increasing concentrations (0.1 μg, 1.0 μg and 10 μg) of IST-9 before mixtures were added to and incubated in the wells with immobilized rScl1 proteins. With increasing concentrations of IST-9 mAb, we show a significant inhibition of binding by both cFn (10–45%) and rEDA (20–54%) to all three rScl1 constructs. These data mapped a Scl1 binding site within the C-C' loop region of EDA, which is also recognized by the $\alpha_9\beta_1$ integrin.

The rScl1*–EDA interaction represents a common cFn-binding mechanism among pathogenically varying GAS strains*

Previous work showed that Scl1 and Scl2 proteins are related but differ in their CL region length and type of triplet repeats used (Xu *et al.*, 2002; Han *et al.*, 2006b). Likewise, phylogenetic tree of the Scl1- and Scl2-V regions revealed that they form two separate branches but are evolutionary related (Han *et al.*, 2006a). The V-region sequences also differ among Scl1 and Scl2 variants found in various GAS strains and they are typically M type-specific (Lukomski *et al.*, 2000a; 2001; Rasmussen *et al.*, 2000; Rasmussen and Björck, 2001; Whatmore, 2001). To date, majority of human ligands bind to Scl1-V but not Scl2-V regions and they display two main binding patterns, e.g. some bind factor H (CFH) and factor H-related protein 1 (CFHR1) (Caswell *et al.*, 2008b; Reuter *et al.*, 2010), whereas other bind low-density lipoprotein (Han *et al.*, 2006a) and ECM components, cFn and Lm (Caswell *et al.*, 2010). To test whether cFn binding via EDA was conserved among Scl1 variants originated from GAS strains of various M types, we examined all previously tested rScl constructs (Caswell *et al.*, 2008b) for binding to rEDA. In this assay, we used the rScl1 proteins, including P144, P161, P176, P186, P190 and P217 that were positive for binding to cFn and Lm, as well as the CFH/CFHR1-binding positive rScl1 proteins P179 and P216. In addition, the rScl2 proteins P163, P177 and P178 were used as ligand-binding negative controls. As shown in Fig. 3A, rScl1 binding to cFn corresponded with binding to rEDA, whereas no binding to pFn by any rScl1 or rScl2 proteins was observed. To test whether all rScl1 constructs bind EDA via the same mechanism, we examined binding of cFn and rEDA in the C-C' peptide inhibition assay described above. The C-C' loop peptide was able to compete with both cFn and rEDA binding to rScl1 proteins, decreasing binding by 50–70%, with no inhibition detected by the scrambled peptide (Fig. 3B). As expected, no additional binding inhibition was observed by the C-C" loop peptide for cFn- and rEDA-binding negative rScl1 and rScl2 proteins. Peptide inhibition results were further strengthened by the IST-9 antibody blocking assay, which was also found to inhibit binding of cFn and rEDA 50% and beyond. The data provide evidence that cFn binding via the C-C' loop region of EDA is conserved among pathogenically varying GAS strains expressing the ECM-binding Scl1 variants.

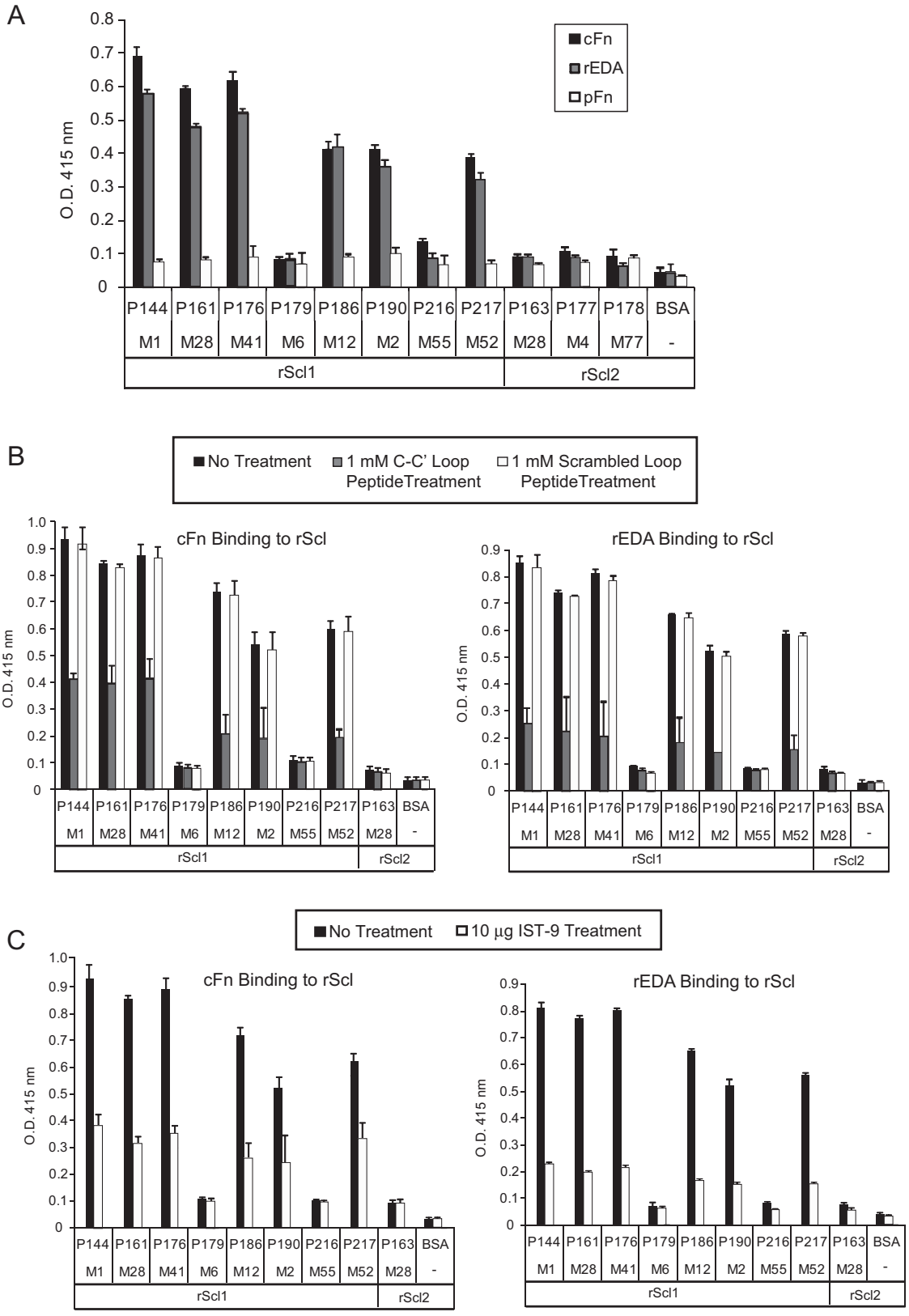
A
O.D. 415 nm
cFn
rEDA
pFn
P144 M1
P161 M28
P176 M41
P179 M6
P186 M12
P190 M2
P216 M55
P217 M52
P163 M28
P177 M4
P178 M77
BSA -
rScl1
rScl2
B
No Treatment
1 mM C-C' Loop PeptideTreatment
1 mM Scrambled Loop PeptideTreatment
cFn Binding to rScl
rEDA Binding to rScl
C
No Treatment
10 μg IST-9 Treatment
cFn Binding to rScl
rEDA Binding to rScl

The Scl1*–ECM interaction supports GAS biofilm formation*

Scl1 proteins have been found to mediate GAS biofilm formation on an abiotic surface (Oliver-Kozup *et al.*, 2011). To assess the importance of the Scl1–cFn interaction in GAS biofilm formation, cell biomass produced by three epidemiologically diverse M41-, M28- and M1-type GAS strains was compared spectrophotometrically following crystal violet staining in an early adhesion (1 h) and mature biofilm (24 h) in untreated or cFn-treated wells (Fig. 4A). M41 wild-type (WT) and the available M41*scl1*-complemented (*scl1*-C) mutant strains form a more robust biofilm at 24 h (OD_{600} ~0.5 untreated vs. ~0.7 cFn-coated), as compared to M28 WT (~0.45 untreated vs. ~0.6 cFn-coated) and M1 WT (~0.23 untreated vs. ~0.34 cFn-coated) strains. Importantly, in each case, more bacterial biomass was detected in cFn-treated wells than on abiotic surface during both the early adherence stage (1 h), as well as in mature biofilms (24 h). Finally, we show a statistically significant decrease in biofilm-forming capacity by all Scl1-negative isogenic mutants as compared to their parent strains at both time points. Confocal laser scanning microscopy of 24 h biofilms confirmed crystal violet staining results (Fig. 4B). The M41 WT biofilm was the most robust with a thickness averaging 26 μm, while a nearly 50% decrease was observed for the M41*scl1* mutant (15 μm). A similar pattern is shown for the M28 WT (22 μm) over the *scl1* mutant (14 μm). The M1-type WT GAS (15 μm) has a decreased capacity for biofilm formation with M1*scl1* mutant (7 μm) poorly supporting a biofilm phenotype. When compared to GAS biofilms formed in untreated (abiotic) wells by the same strains (Oliver-Kozup *et al.*, 2011), cFn-mediated biofilms were enhanced up to 40% in average thickness recorded for WT strains. Collectively, we can conclude from these studies that Scl1-mediated binding of GAS to cFn significantly enhances biofilm formation.

Scl1*-mediated binding to fibroblast-derived ECM supports GAS adherence and biofilm formation*

To develop a system that allows biofilm development on ECM more closely mimicking the ECM in tissue *in vivo*, normal human dermal fibroblasts (HDFa) were used to deposit ECM. To generate the fibroblast-derived ECM (fdECM), wells were denuded of HDFa cells and the presence of fdECM was visualized by Ponceau S staining (Fig. S1A). When the composition of fdECM coating was characterized by ELISA using antibodies that detect ECM proteins, Fn and collagens were identified as major constituents (Fig. S1B). Importantly, we detected the presence of the EDA/cFn variant within fdECM using the mAb, IST-9. Thus, we confirmed that fdECM coating provides a more complex model of tissue matrix compared to single ECM component, which includes the EDA/cFn population recognized by Scl1, a streptococcal adhesin.

Group A *Streptococcus* strains used in this study express varying numbers of surface adhesins, including Fn-binding adhesins. The fdECM matrix contains a number of ECM components assembled into a higher-ordered structure more suitable for assessing whether Scl1–EDA/cFn binding significantly contributes to the adherence and biofilm formation by epidemiologically varying GAS strains. The structural complexity of the fdECM network was demonstrated by field emission scanning electron microscopy (FESEM) [Fig. 5A, row (i)]. Using FESEM to image GAS adherence on a fdECM coating, WT GAS strains of M1- (ii), M28- (iii) and M41-type (iv) were observed to be targeted or preferentially bound to fdECM deposits, as compared to the surrounding abiotic surface at early time points in infection. At higher magnification, GAS chains are observed in close contact with fdECM fibrous structures. When GAS WT and *scl1*-inactivated mutant strains were compared based on crystal violet staining for bacterial biomass after 1 h (adherence) and 24 h (mature biofilm) on fdECM, or cFn-coated wells, GAS–fdECM binding produced comparable biofilm absorbance values to those of the cFn-treated wells (Fig. 5B). Scl1-negative isogenic mutants had decreased capacity for adherence and mature biofilm formation, as compared to their WT parent strains, on both ECM-treated wells. Our findings demonstrated that the Scl1 protein plays a significant role in GAS biofilm formation on a single cFn coating, as well as on a more complex fdECM, for all strains tested.

Experiments shown in Figs 2 and 3 demonstrated that we can significantly inhibit rScl1 binding to both rEDA and cFn using the synthetic C-C' loop peptide or IST-9 mAb. Here, we adapted both inhibition assays in order to evaluate the importance of the interactions between native Scl1 surface protein and EDA/cFn component of fdECM in total GAS adherence (Fig. 6). Graphs represent spectrophotometric measurements following crystal violet staining (OD_{600} values) obtained for each WT strain (M41, M28 and M1) on all three ECM coatings (cFn, rEDA, fdECM) in wells without inhibitors and in wells treated with either the C-C' loop peptide (Fig. 6A) or IST-9 mAb (Fig. 6B). Below the graphs, we present these OD_{600} value data as per cent (%) adherence inhibition, as compared with their corresponding untreated samples (100% adherence). For comparison, we also present % adherence inhibition, resulting from genetic inactivation, of their corresponding untreated *scl1* mutants (OD_{600} values are shown in Fig. S2). First, the C-C' loop or scrambled peptide (1 mM each) were added to GAS WT (Fig. 6A) or *scl1* mutant strains (Fig. S2A). Next, peptide–GAS mixtures were added to ECM-coated wells and 1 h adherence was analysed

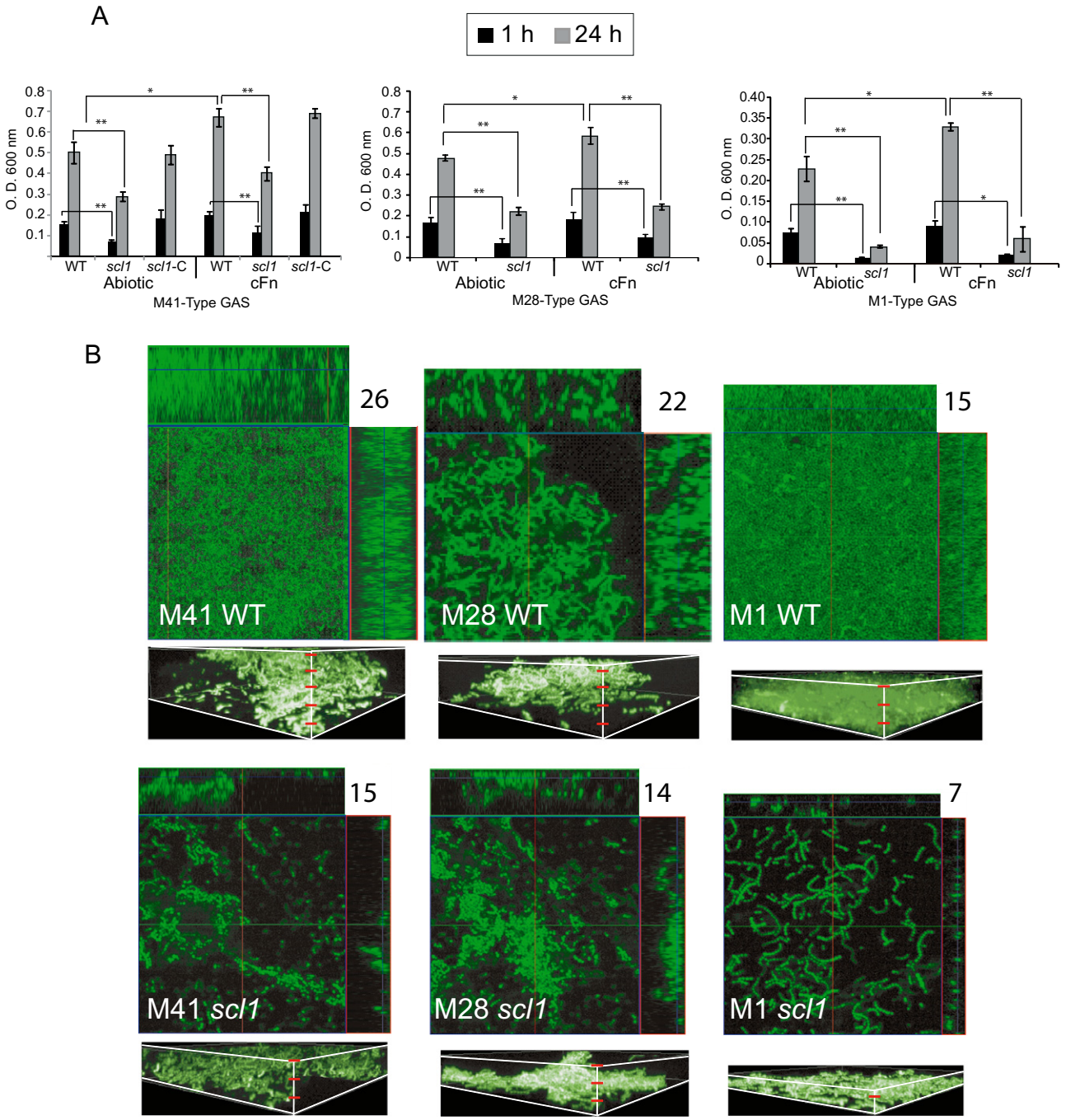

Fig. 4. Scl1–cFn binding mediates and enhances biofilm formation by GAS. WT GAS strains M41-, M28- and M1-type, their *scl1*-inactivated isogenic mutants (M41*scl1*, M28*scl1*, M1*scl1*), and the M41*scl1*-C mutant strain complemented *in-trans* for Scl1.41 expression were compared for biofilm formation.

A. Biofilm formation on abiotic or cFn-coated surface. Biofilm formation for each GAS strain was evaluated spectrophotometrically following crystal violet staining. Graphic bars indicate the mean $OD_{600\ nm}$ normalized against BSA controls. Statistical analysis was computed from three independent experimental repeats, each performed in triplicate wells ($n = 3 \pm$ SD); $^{*}P \leq 0.05$, $^{**}P \leq 0.001$.

B. Analysis of biofilms formed on cFn-coated surface using confocal laser scanning microscopy. GAS strains were transformed with the GFP-encoding plasmid and grown on cFn-coated glass coverslips for 24 h. Two-dimensional orthogonal views of GAS biofilms are representative of Z-stacks from 10 fields within a single experiment. Average vertical thickness is indicated in micrometres. Conversion to three-dimensional images was performed with conventional Z-stacks, deconvoluted stepwise using AutoQuant, and transformed using NIS-element software. Nick marks represent 5 μm in thickness and averages were taken from 10 fields within a single experiment.

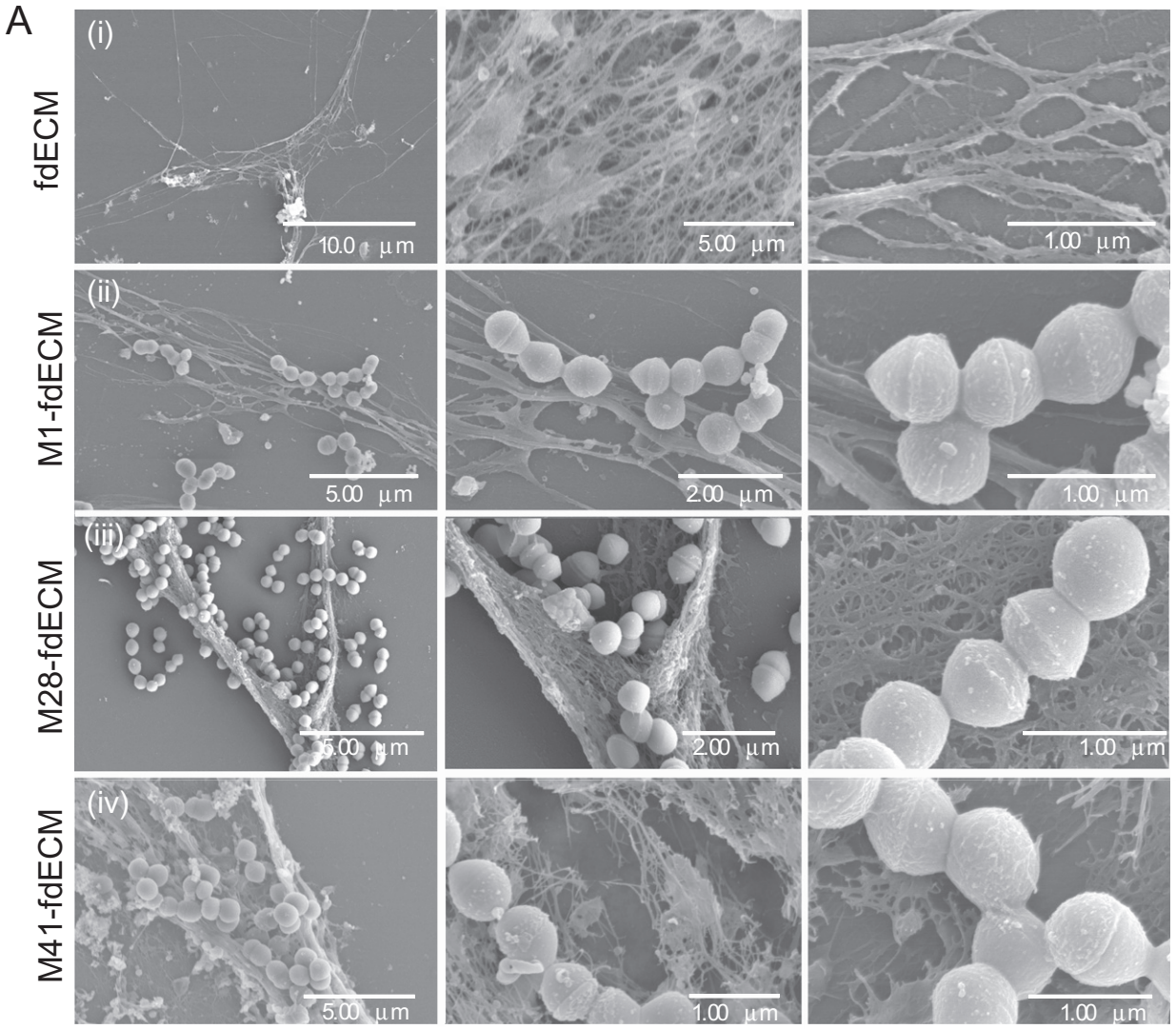
A
fdECM
M1-fdECM
M28-fdECM
M41-fdECM
(i)
(ii)
(iii)
(iv)
10.0 µm
5.00 µm
1.00 µm
5.00 µm
2.00 µm
1.00 µm
5.00 µm
2.00 µm
1.00 µm
5.00 µm
1.00 µm
1.00 µm

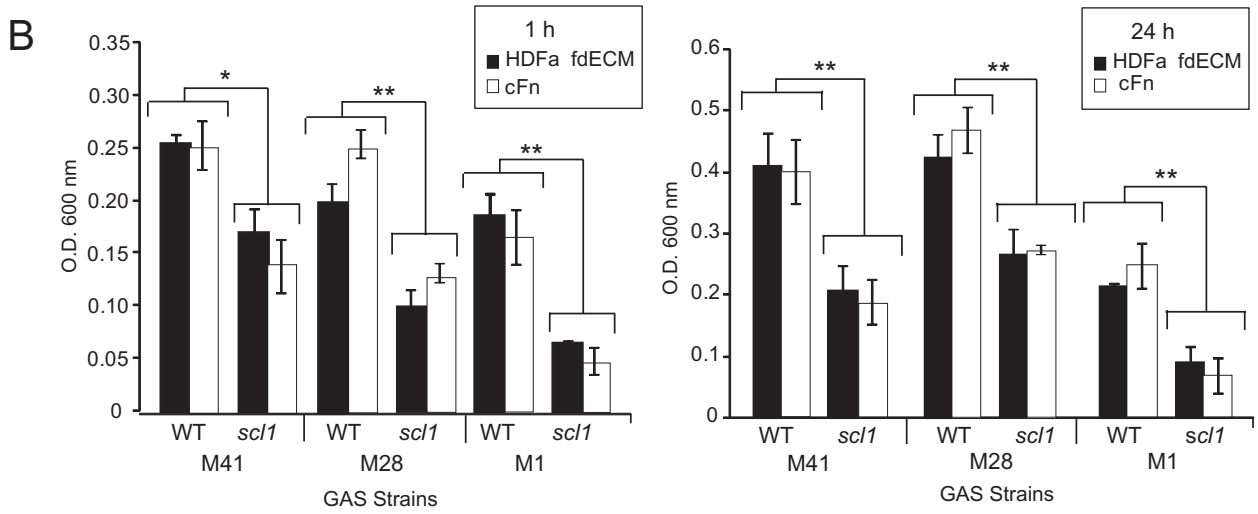
B
1 h
HDFa fdECM
cFn
O.D. 600 nm
0.35
0.30
0.25
0.20
0.15
0.10
0.05
0
*
**
**
WT
scl1
WT
scl1
WT
scl1
M41
M28
M1
GAS Strains
24 h
HDFa fdECM
cFn
O.D. 600 nm
0.6
0.5
0.4
0.3
0.2
0.1
0
**
**
**
WT
scl1
WT
scl1
WT
scl1
M41
M28
M1
GAS Strains

Fig. 5. Scl1 binding to ECM derived from human dermal fibroblasts (HDFa) mediates and enhances biofilm formation by GAS. Adult normal HDFa were grown to confluency, detached by EGTA treatment and removed from the wells. GAS adherence to fibroblast-deposited ECM (fdECM) was analysed using field emission scanning electron microscopy (FESEM) and overall biofilm formation on fdECM and cFn were compared spectrophotometrically following crystal violet staining.
A. Adherence of WT GAS to fdECM by FESEM. GAS strains were grown for 2 h on HDFa-deposited fdECM to analyse the early adherence stage in biofilm formation. FESEM images were taken with increasing magnification (left to right). Scale bars are indicated in micrometres. Row (i): images depict acellular fibrous network of deposited fibroblast-derived matrices. Rows (ii–iv): adherence of M1- (ii), M28- (iii) and M41-type (iv) GAS strains to deposited fdECM is observed.
B. fdECM supports Scl1-mediated GAS biofilm formation. WT M41-, M28- and M1-type GAS strains and their *scl1*-inactivated isogenic mutants were tested for initial adherence (1 h) and mature biofilm (24 h) in wells primed with either fdECM or with commercial cFn. Graphic bars indicate the mean $OD_{600\ nm}$ normalized against BSA controls. Statistical analysis was computed from three independent experimental repeats, each performed in triplicate wells ($n = 3 \pm$ SD); $^{*}P \leq 0.05$, $^{**}P \leq 0.001$.

spectrophotometrically following crystal violet staining. The adherence of all WT strains was significantly inhibited on all three coatings, whereas adherence of *scl1*-inactivated mutants was unaffected by peptide treatment (Fig. S2). Inhibition levels of adherence obtained for peptide-treated strains type M41 and M28 were similar, ranging on assorted ECM coatings between 25% and 27% of their untreated samples. The remaining binding levels (as well as % inhibition values) were similar to the binding levels of untreated Scl1-negative mutant strains, ranging between 24% and 28%, which is depicted in the graph by horizontal lines over-imposed on bars representing untreated samples. Interestingly, a 25–33% C-C' peptide inhibition range was also measured for the M1 WT strain; however, the binding-inhibition levels obtained for the M1-*scl1* mutant on assorted ECM coatings were substantially higher (51–54%). No strains were inhibited by treatment with the scrambled peptide (data not shown).

In a second set of inhibition studies (Figs 6B and S2B), ECM-coated wells were pre-treated with 10 μg of mAb IST-9 for 1 h followed by the addition of GAS strains. Again, 1 h adherence was analysed spectrophotometrically following crystal violet staining. Similar to the peptide inhibition described above, we identified a statistically significant decrease in adherence by M41 and M28 WT strains treated with IST-9 mAb (24–30% range) and, again, the remaining binding levels of these IST-9-treated samples were similar to the binding levels of their untreated Scl1-negative mutants (25–32%). As previously shown, by comparison, the M1 *scl1* mutant had substantially decreased adherence on all three ECM coatings (50–60% inhibition), whereas adherence inhibition of the M1 WT strain due to IST-9 treatment was lower (32–35%). In total, inhibition studies demonstrate that GAS adherence to ECM substrates, including complex fdECM network, can be abrogated with treatments that target the integrin-binding C-C' loop region of the EDA/cFn.

Discussion

The skin is an organ covering the human body that forms an effective barrier between the internal and external environments and protects against invading microbes (Holbrook and Smith, 2002). GAS is, together with *Staphylococcus aureus*, a predominant pathogen of the skin and soft tissue (Bisno *et al*., 2005; Tognetti *et al*., 2012). GAS, as well as other bacteria, requires a portal of entry to initiate the infection. In the wounded site, GAS faces a new environment, which creates a unique opportunity for adhesion to the host's cellular and extracellular components via surface adhesins designated MSCRAMMs for 'microbial surface components recognizing adhesive matrix molecules' (Patti *et al*., 1994). Among various MSCRAMMs expressed by GAS strains (Chhatwal and Preissner, 2000), Scl1 was recently shown to selectively bind cFn (Caswell *et al*., 2010). Here, we characterize Scl1–cFn interactions and investigate the role of this binding in GAS-ECM adherence and biofilm formation on single ECM coatings and on complex ECM structures deposited by human cells.

In the present study, we selected three model GAS strains representing the intraspecies breadth. The M1-type strain represents the global M1T1 clone responsible for pharyngitis and invasive infections (Sumby *et al*., 2005; Aziz and Kotb, 2008), the M28-type strain has been historically associated with puerperal sepsis (Green *et al*., 2005a,b; O'Loughlin *et al*., 2007), and the M41-type strain has been predominantly linked to skin infections (Anthony *et al*., 1967; Dillon and Wannamaker, 1971; Dillon *et al*., 1974). Importantly, these strains vary in the number of Fn-binding proteins they express in addition to Scl1 (Caswell *et al*., 2007). The M28-type strain harbours at least three genes encoding known Fn-binding proteins, including the serum opacity factor (*sof*) (Courtney *et al*., 1999; Katerov *et al*., 2000; Oehmcke *et al*., 2004), *prtF1*/*sfb*I (Hanski and Caparon, 1992) and *prtF2*/*pfbp* (Jaffe *et al*., 1996; Rocha and Fischetti, 1999). M41-type strain has the *prtF2/pfbp* gene, whereas the M1-type strain has none of them. Based on this knowledge, the contribution of each Scl1.1, Scl1.28 and Scl1.41 variant to the attachment and biofilm formation on single cFn and complex fdECM coatings by these strains was tested.

First, we investigated the selective recognition of and binding to cFn by rScl1 proteins. There is a large body of

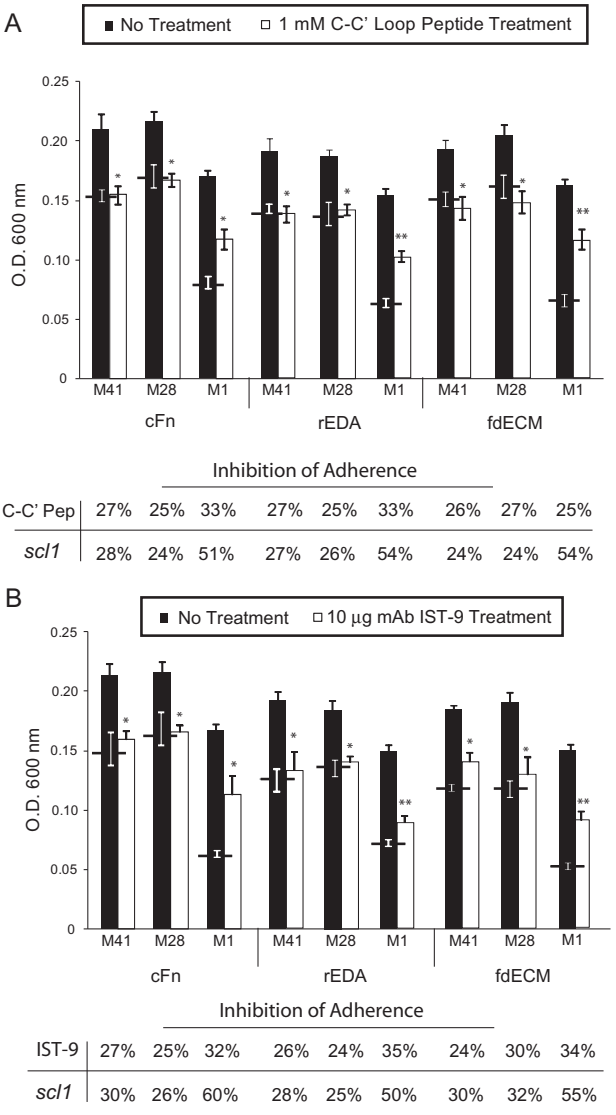

Fig. 6. Inhibition of GAS adhesion by targeting the C-C' loop of EDA. Spectrophotometric analysis following crystal violet staining at 1 h is shown. Black solid horizontal lines over-imposed on bars showing untreated samples of GAS WT strains represent adhesion values of the corresponding untreated *scl1*-inactivated mutant strains (shown in Fig. S2). Graphic bars indicate the mean $OD_{600\ nm}$ normalized against BSA controls. Statistical analysis was computed from three independent experimental repeats, each performed in triplicate wells ($n = 3 \pm$ SD); $^{*}P \leq 0.05$, $^{**}P \leq 0.001$.
A. Inhibition of GAS adhesion with synthetic C-C' loop peptide. M1-, M28- and M41-WT GAS strains were pre-treated with the exogenous C-C' loop peptide or a scrambled loop peptide (not shown) and then added to ECM-coated wells. Below the graph, we present these $OD_{600\ nm}$ value data as per cent (%) adherence inhibition, as compared with their corresponding untreated samples (100% adherence).
B. Inhibition of GAS adhesion by mAb IST-9. ECM-coated wells were pre-treated with mAb IST-9 followed by the addition of GAS strains. Below the graph, we present % adherence inhibition, resulting from genetic inactivation, of their corresponding untreated *scl1* mutants (OD_{600} values are shown in Fig. S2).

literature describing redundancy in Fn binding by GAS surface proteins (Henderson *et al.*, 2011). They are often closely related among Gram-positive bacteria or contain related regions that are involved in Fn binding (Patti *et al.*, 1994) and include GAS proteins M, F1/SfbI, SfbII, F2/PFBP, SOF, FBP54 and FbaA and B (Talay *et al.*, 1994; Kreikemeyer *et al.*, 1995; 2004; Jaffe *et al.*, 1996; Courtney *et al.*, 1999; Cue *et al.*, 2001; Terao *et al.*, 2001; 2002). Unlike Scl1, these proteins bind pFn and subsequent studies mapped their binding sites within the N-terminal region spanning type I and type II repeats of Fn, which is identical in pFn and cFn (Ozeri *et al.*, 1998; Ensenberger *et al.*, 2001; Courtney *et al.*, 2003; Bingham *et al.*, 2008; Margarit *et al.*, 2009). The cFn isoforms differ from pFn in that they include in varying proportions the extra domains, termed EDA/EIIIA and EDB/EIIIB (Pankov and Yamada, 2002). In the wound, platelets are activated, degranulate and release EDA-containing Fns into the apical aspect of the fibrin matrix in the region that is first encountered by microorganisms (Sakai *et al.*, 2001). Within 2 days wound macrophages and fibroblasts produce cFns rich in the EDA segment and these cFns persist throughout the wound bed for at least a week following injury (Brown *et al.*, 1993). Using peptide inhibition and antibody blocking experiments, we demonstrated that multiple rScl1 proteins bind cFn via the C-C' loop region of EDA, indicating a common binding mechanism among pathogenically discrete strains. Thus, we have identified a novel Fn-binding mechanism unique to Scl1, which allows GAS to target the EDA/cFn spliced variant expressed in wounded tissue.

Within hours of injury, neutrophils populate the wound and thereafter macrophages arrive and epidermal keratinocytes commence migration over the provisional matrix (Martin, 1997). These cells express integrins that bind the EDA/cFn, including $\alpha_9\beta_1$ (Taooka *et al.*, 1999). The C-C' loop region of EDA domain mediates binding to $\alpha_9\beta_1$ and $\alpha_4\beta_1$ integrins (A. V. Shinde and L. Van De Water, unpubl. obs.) and has been shown to participate in cell adhesion, cell spreading (Shinde *et al.*, 2008) and matrix assembly (Bazigou *et al.*, 2009). Aberrations in, or blocking of, the C-C' loop region in EDA abrogate the EDA–integrin binding (Liao *et al.*, 2002; Shinde *et al.*, 2008). Our current binding-inhibition studies, as well as preliminary cell-attachment inhibition assays (not shown), demonstrated that rScl1 binds to the C-C' functional loop region of EDA, which is also the integrin-binding site. This implies that during GAS infection, the Scl1 adhesin could abrogate human cell migration and adhesion, thus impairing wound healing. Interestingly, a recent study showed that reepithelialization of a murine cutaneous wound was delayed by staphylococcal infections (Schierle *et al.*, 2009). Considering the overall similarities between streptococcal and staphylococcal skin

infections, it is tempting to speculate that GAS evolved analogous molecular mechanisms that augment tissue colonization by manipulating the local host's environment at the site of infection.

Group A *Streptococcus* biofilm is a relatively new concept (Lembke *et al*., 2006), which is increasingly being established with supporting data collected from clinical specimens (Akiyama *et al*., 2003) and through animal model research (Roberts *et al*., 2010; Connolly *et al*., 2011). Several GAS surface components have been reported to participate in biofilm formation (Cho and Caparon, 2005; Manetti *et al*., 2007; Courtney *et al*., 2009; Maddocks *et al*., 2011; Kimura *et al*., 2012) including the Scl1 protein (Oliver-Kozup *et al*., 2011). In the latter study, we reported that Scl1 plays a substantial role in GAS biofilm formation on an abiotic surface. We also proposed a model in which Scl1–ECM binding enhances biofilm formation by anchoring the growing biofilm structure. Here, we tested that model by assessing the significance of one interacting component, Scl1–cFn binding in the formation of GAS biofilm. Direct comparison of biofilms grown by the M1-, M28- and M41-type strains showed a significantly increased biofilm biomass on cFn-coated surface compared to an inanimate surface. These differences were further confirmed microscopically as the average thickness of mature biofilms formed by each of these strains was higher on cFn coating by up to 40%. However, these results could also be explained by the non-Scl1-mediated interactions between cFn and other Fn-binding MSCRAMMs expressed by these strains. Therefore, a similar comparison was made between biofilms formed by the WT and isogenic *scl1*-inactivated mutants of each M-type strain on cFn coating. Despite the presence of additional Fn-binding proteins, especially in M28- and M41-type strains, that bind a different region of Fn, all Scl1-devoid mutants produced significantly lower biofilm biomass and lower biofilm thickness by nearly 50%, suggesting an important role for the Scl1–EDA interaction.

The complexity of natural ECM in tissue exceeds the single cFn coating we initially employed. Therefore, we developed a more complex fdECM coating, which was denuded of cells. Following eukaryotic cell removal, tissue culture wells contained a complex 2-D fibrillar network composed of several ECM components, including various collagens and laminin in addition to the EDA/cFn isoforms within Fn. A similar approach was used to study the attachment and biofilm formation of *Klebsiella pneumoniae* on coating derived from ECM deposited by bronchial epithelial cells (Jagnow and Clegg, 2003). This coating produced a rich biofilm phenotype that was more versatile as compared to a collagen coating or an abiotic surface. In our hands, complex fdECM supported WT GAS adherence and biofilm formation at the levels comparable with cFn coating. Scanning electron microscopy revealed targeted or preferential GAS binding to fdECM structures over the surrounding abiotic area. The *scl1* isogenic mutants showed significantly decreased adherence and biofilm formation on fdECM similarly to that on cFn-treated wells. Furthermore, we were able to reduce the adherence of the WT strains to the levels shown by the *scl1* mutants with the C-C' loop peptide and mAb IST-9. The importance of Scl1–EDA/cFn binding in GAS adherence on fdECM was intriguing, considering the fact that GAS cells are equipped with more than one Fn-binding protein and, likely, with more than one type of MSCRAMM targeting additional components of fdECM. As inhibition was not complete, our data also point at the contribution and importance of other adhesins and alternative ECM-binding mechanisms to GAS adherence and host colonization.

In summary, we characterized Scl1–cFn interactions and mapped the Scl1 binding site within the functional C-C' loop region of the EDA segment overlapping with the $\alpha_9\beta_1$-integrin binding site. This observation opens new directions of investigations as $\alpha_9\beta_1$ is expressed by a number of epithelial and inflammatory cells involved in tissue repair and wound healing (Palmer *et al*., 1993; Taooka *et al*., 1999; Singh *et al*., 2004; 2009). We studied the contribution of Scl1–ECM adhesion in GAS biofilm formation on a single cFn coating and on complex fdECM 2-D matrix. Based on these results, we propose a model of the Scl1-mediated tissue colonization by GAS (Fig. 7). In this mechanistic model, the opportunistic GAS pathogen exploits injured tissue as a portal of entry to establish skin infection. Within injured site, platelets, macrophages and underlying injured fibroblasts deposit in the wound bed a provisional ECM matrix, which includes the EDA-enriched cFn to provide scaffolding for cell migration and proliferation via $\alpha_9\beta_1$, $\alpha_4\beta_1$ and $\alpha_4\beta_7$ integrins, and promote structural remodelling and tissue repair (Humphries *et al*., 2006). Upon entry into the injured site, GAS utilizes the Scl1 protein to initiate binding to the EDA domain of cFn, which is mediated via the C-C' loop region and secures adherence to ECM, facilitating microcolony formation. Scl1 acts in concert with other GAS adhesins that, depending on strain, may include Fn-binding proteins M, F1/SfbI, SfbII, F2/PFBP, SOF, FBP54 and FbaA and B (Schmidt *et al*., 1993; Talay *et al*., 1994; Kreikemeyer *et al*., 1995; 2004; Jaffe *et al*., 1996; Courtney *et al*., 1999; Cue *et al*., 2001; Terao *et al*., 2001; 2002). The Scl1–EDA binding may also compete with EDA binding by the integrins expressed on migrating keratinocytes, thus delaying wound reepithelialization and healing. Growing GAS microcolonies form a focused nidus of tissue infection until it is overcome by immune defences or disperses to new superficial or deep tissue sites. Validation of this updated model is ongoing research.

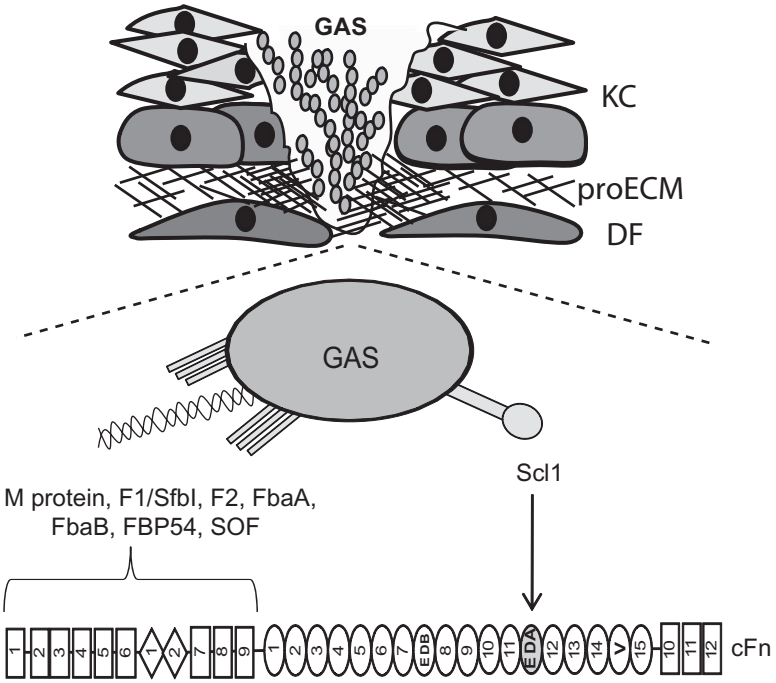

Fig. 7. A model of Scl1-mediated wound colonization by GAS. (Upper schematic) Initiation of GAS infection requires a skin infringement or portal of entry. During tissue repair, host cells deposit in the wound bed a provisional ECM matrix, which includes the EDA-enriched cFn to provide scaffolding for cell migration and proliferation through integrin binding, and functions to promote the wound healing process. (Lower schematic) GAS utilizes the Scl1 protein for targeted binding to the EDA domain of cFn. This Scl1 binding to EDA/cFn variant promotes GAS attachment and colonization of the wound in concert with other GAS adhesins that bind the N-terminal region of Fn. KC, keratinocytes; proECM, provisional extracellular matrix; DF, dermal fibroblasts.

Experimental procedures

Bacterial strains and growth

The M41- (MGAS 6183), M28- (MGAS 6143) and M1-type (MGAS 5005) strains of GAS were used. All GAS cultures were grown at 37°C in an atmosphere of 5% CO_2–20% O_2. For biofilm formation, GAS strains were grown overnight on brain–heart infusion agar (BHI) (BD Biosciences) and used to inoculate Todd-Hewitt broth (Difco) supplemented with 0.2% yeast extract (THY medium). Cultures were incubated until they reached logarithmic phase (OD_{600} ~0.5) and used to inoculate treated or untreated tissue culture wells.

Construction of scl1-inactivated mutants

The isogenic Scl1-negative mutants for all WT strains were constructed by allelic replacement as described previously. Briefly, the *scl1* gene in M1-type strain was inactivated using the suicide plasmid, pSL134, harbouring the *scl1.1* allele with flanking regions and non-polar spectinomycin resistance cassette, spc2, inserted in-frame to replace the *scl1.1* coding region (Lukomski *et al*., 2000b). The *scl1.28* and *scl1.41* alleles were inactivated using the pSL170 suicide plasmid containing the erythromycin-resistant *scl1.*28::erm2 construct (Han *et al*., 2006a; Caswell *et al*., 2007). WT strains were electroporated followed by incubation in THY medium for 2.5 h. Cultures were then plated onto BHI agar containing either 100 μg ml^{-1} spectinomycin or 3 μg ml^{-1} erythromycin. Drug-resistant transformants were initially screened by PCR for amplified single products, indicating double cross-over recombination, and were subsequently confirmed by DNA sequencing. For complementation of the *scl1.41*-inactivated mutant, the MGAS 6183 *scl1*-mutant cells were electroporated with the plasmid construct pSL230 encoding the Scl1.41 protein (Caswell *et al*., 2007). Scl1 expression or lack of it was confirmed by Western immunoblotting.

Recombinant proteins

Several *scl1* and *scl2* alleles encoding the extracellular protein portion were amplified by PCR and cloned into the pASK-IBA2 vector designed for periplasmic protein expression (Xu *et al*., 2002; Humtsoe *et al*., 2005; Han *et al*., 2006a,b; Caswell *et al*., 2007). Recombinant Scl1 and Scl2 (rScl) proteins used in these assays: P144/rScl1.1 (accession no. AF252861), P161/Scl1.28 (accession no. AY459361), P176/rScl1.41 (accession no. AY452037), P179/rScl1.6 (accession no. EU 127997) P186/rScl1.12 accession no. DQ309441), P190/rScl1.2 (accession no. EU127996), P216/rScl1.55 (accession no. EU127999), P217/rScl1.52 (accession no. EU127998), P163/rScl2.28 (accession no. AY069936), P177/rScl2.4 (accession no. DQ309442), P178/rScl2.77 (accession no. DQ309443). All rScl proteins contain short C-terminal tag, the *Strep*-tag II (WSHPQFEK), which has high binding affinity to *Strep*-Tactin-Sepharose for affinity chromatography purification (IBA-GmbH, Goettingen, Germany). *Escherichia coli* DH5α and BL21 strains were used for cloning and protein expression respectively.

The his-tagged rEDA and rIII4 polypeptides were prepared as described (Liao *et al*., 1999). Briefly, EDA or III4 cDNA was amplified by PCR, cloned into plasmid pGEX-2T, expressed in *E. coli*, and purified using affinity chromatography nickel columns.

Protein binding assays

For binding studies, rScl proteins (0.5 μM) were immobilized onto *Strep*-Tactin-coated microplate wells for 1.5 h at room temperature and blocked with Tris-buffered saline (TBS) sup-

plemented with 1% bovine serum albumin (BSA) overnight at 4°C followed by incubation with the ECM proteins cFn, rEDA, and rIII4 or pFn (Sigma). The no rScl controls were performed in BSA-coated wells for each ligand and each antibody used. Final ODs were normalized by subtracting the BSA controls in each experimental set-up.

All ECM ligands prepared at 0.25 μM concentration for binding inhibition studies or 1 μg of ECM ligand per well for protein screening experiments were added to rScl-immobilized wells in triplicate and incubated at room temperature for 1 h. Bound ligands were detected with specific anti-cFn (Sigma) and anti-collagen I, -collagen II, -collagen IV primary antibodies and goat-anti-rabbit secondary antibodies conjugated to horseradish peroxidase (HRP) (Bio-Rad). The HRP substrate, 2,20-azino-bis(3-ethylbenzthiazoline-6-sulphonic acid) was used and colorimetric reaction was recorded at $OD_{415\ nm}$.

For peptide inhibition studies, synthetic 11-amino-acid peptide representing the C-C' loop region of the EDA domain (TYSSPEDGIHE) or a scrambled loop peptide (SEDIHYTEGPS) were used (LifeTein). rScl proteins (0.5 μM) were immobilized onto *Strep*-Tactin-coated wells as above and were either untreated or pre-incubated with increasing concentrations (0.01–1.0 mM) of the synthetic C-C' loop EDA peptide or scrambled peptide for 30 min to 1 h at room temperature. cFn or rEDA ligands were next added to the wells and incubated at room temperature for 1 h. Bound ECM ligands were detected with specific primary and HRP-conjugated secondary antibodies as above.

For antibody inhibition studies, the mAb IST-9 was used, which recognizes the Ile[43] and His[44] epitope (Liao *et al*., 1999) within the C-C' loop region of EDA. ECM ligands (0.25 μM) were pre-incubated with increasing concentrations (0–10 μg) of the IST-9 mAb for 30 min at room temperature. Mixtures were added to rScl1-immobilized wells and bound ECM ligands were detected as above with specific primary and HRP-conjugated secondary antibodies.

Analysis of biofilm formation

Crystal violet staining assay. Untreated or pre-treated tissue culture polystyrene 24-well plates were used to assess biofilm formation. ECM-coated wells were pre-treated with cFn, rEDA or 1% BSA in TBS overnight at 4°C and then blocked for 2 h with 1% BSA in TBS at room temperature. Exponential-phase GAS cultures (0.5 ml) were seeded into untreated or treated wells and incubated at 37°C in an atmosphere of 5% CO_2–20% O_2. Medium was removed at 1 h or 24 h and wells were washed with PBS followed by the addition of 0.5 ml of 1% (v/v) solution of crystal violet reagent (Becton Dickinson) in PBS, and incubation at room temperature for 30 min. Biomass staining was solubilized with 0.5 ml of ethanol and spectrophotometric readings were recorded at $OD_{600\ nm}$ for each sample at each time point. Statistical analysis is reported based on three independent experimental repeats ($n = 3 \pm$ SD) with triplicate technical replicates in each experiment. Statistical significance was denoted as $^{*}P \leq 0.05$ and $^{**}P \leq 0.001$.

Adherence inhibition studies. For inhibition of biofilm formation both synthetic C-C' loop peptide and IST-9 mAb were used. GAS WT and mutant strains were grown to logarithmic phase and pre-incubated with 1 mM synthetic C-C' loop or scrambled peptide. Then, 0.5 ml of the mixture was added to ECM-treated wells in triplicate and incubated at 37°C in an atmosphere of 5% CO_2–20% O_2. Adherence inhibition at 1 h was analysed spectrophotometrically following crystal violet staining. For antibody inhibition assay, ECM-treated wells were pre-incubated with mAb IST-9 (10 μg) for 1 h at room temperature. Wells were then washed with PBS to remove unbound antibody. 0.5 ml of logarithmic-phase GAS WT and mutant strains were added to triplicate wells and incubated at 37°C in an atmosphere of 5% CO_2–20% O_2. Bacterial biomass was measured spectrophotometrically after 1 h following crystal violet staining. Statistical analysis is reported based on three independent experimental repeats ($n = 3 \pm$ SD) with triplicate technical replicates in each experiment. Statistical significance was denoted as $^{*}P \leq 0.05$ and $^{**}P \leq 0.001$.

Microscopy techniques

Confocal laser scanning microscopy. To visualize GAS cells by confocal laser scanning microscopy, GAS WT and *scl1*-inactivated mutants were transformed with plasmid pSB027 (Cramer *et al*., 2003; Caswell *et al*., 2010; Oliver-Kozup *et al*., 2011) to express green fluorescent protein (GFP). GAS cells grown to $OD_{600\ nm}$ ~0.5 were inoculated onto untreated or cFn-coated 15 mm glass coverslips placed into 24-well tissue culture plate wells and incubated for 24 h. Biofilms were washed gently with PBS and fixed with 3% paraformaldehyde in PBS at room temperature for at least 2 h. Coverslips were mounted to slides using Prolong Gold (Invitrogen). Fluorescent images were acquired using the confocal microscope (LSM 510 Carl Zeiss) equipped with a 63×/1.40 Oil Plan-Apochromatic objective. Z-stack profiles were further deconvoluted stepwise by AutoQuant software at 0.36 μm and were visualized as three-dimensional images using NIS – Elements software. Additional visualization was performed using the Zeiss trinocular EPI fluorescence microscope equipped with four achromatic objectives. The Zeiss AxioCam Mrc5 camera and Zeiss AxioVision 4.8 software were used for image acquisition.

Field emission scanning electron microscopy. GAS biofilm samples were prepared and fixed as above. The samples were post-fixed in osmium tetroxide, dehydrated in an ethanol series, and dried using hexamethyldisilazane. Samples were mounted onto aluminium stubs, sputter-coated with gold/palladium, and imaged on a Hitachi S-4800 field emission scanning electron microscope as previously reported (Oliver-Kozup *et al*., 2011).

Cell culture techniques

fdECM production and analysis. Adult HDFa were grown in Medium 106 (Invitrogen) supplemented with low serum growth supplement to confluency at 37°C in an atmosphere of 5% CO_2. For fdECM production, HDFa were grown on sterile 15 mm glass coverslips inserted into wells. Cells were removed by treatment with 2 mM ethylene glycol tetraacetic

acid, leaving naturally deposited network of ECM. Samples were washed gently with PBS and fixed with 3% paraformaldehyde for at least 2 h or overnight, and analysed microscopically following Ponceau S staining or by FESEM. ELISA was performed to determine the presence of ECM components: total cFn, EDA-containing cFn, collagens type I, II and IV, and laminin. Components present were detected with specific primary antibodies: anti-Fn (Sigma), anti-EDA/cFn (IST-9: Santa Cruz Biotechnology), anti-collagens I, II, IV (Chemicon/Millipore) and anti-laminin (Sigma). Appropriate secondary antibodies conjugated to HRP (Bio-Rad) were used and developed with ABTS substrate.

Statistical analysis

Statistical analysis was performed using the two-tailed paired Student's *t*-test and significance was denoted at a level of $^{*}P \leq 0.05$ or $^{**}P \leq 0.001$. Error bars represent standard deviations with analyses based on three independent experimental repeats ($n = 3$), each performed in triplicate technical replicates.

Acknowledgements

We thank Joan Olson and Fred Minnear for the critical reading of the manuscript. The support of Xin-Xing Gu is greatly appreciated. This work was supported in part by National Institutes of Health Grant AI50666 (to S. Lukomski) and GM056442 (to L. Van De Water). Authors also wish to acknowledge the WVU Research Office's Program to Stimulate Competitive Research (PSCoR), as well as the Research Funding Development Grant (RFDG) (to S. Lukomski). H. Oliver-Kozup was supported by a grant from the West Virginia Graduate Student Fellowship in Science, Technology, Engineering and Mathematics (STEM). Confocal microscopy experiments were performed in the West Virginia University Microscope Imaging Facility, which has been supported by the Mary Babb Randolph Cancer Center and NIH grants P20 RR016440, P30 RR032138/GM103488 and P20 RR016477. The findings and conclusions in this report are those of the authors and do not necessarily represent the views of the National Institute of Occupational Safety and Health.

References

Akiyama, H., Morizane, S., Yamasaki, O., Oono, T., and Iwatsuki, K. (2003) Assessment of *Streptococcus pyogenes* microcolony formation in infected skin by confocal laser scanning microscopy. *J Dermatol Sci* **32:** 193–199.

Almengor, A.C., Walters, M.S., and McIver, K.S. (2006) Mga is sufficient to activate transcription in vitro of *sof-sfbX* and other Mga-regulated virulence genes in the group A *Streptococcus*. *J Bacteriol* **188:** 2038–2047.

Anthony, B.F., Perlman, L.V., and Wannamaker, L.W. (1967) Skin infections and acute nephritis in American Indian children. *Pediatrics* **39:** 263–279.

Aziz, R., and Kotb, M. (2008) Rise and persistence of global M1T1 clone of *Streptococcus pyogenes*. *Emerg Infect Dis* **14:** 1511–1517.

Bazigou, E., Xie, S., Chen, C., Weston, A., Miura, N., Sorokin, L., *et al.* (2009) Integrin-α_9 is required for fibronectin matrix assembly during lymphatic valve morphogenesis. *Dev Cell* **17:** 175–186.

Bingham, R.J., Rudino-Pinera, E., Meenan, N.A., Schwarz-Linek, U., Turkenburg, J.P., Höök, M., *et al.* (2008) Crystal structures of fibronectin-binding sites from *Staphylococcus aureus* FnBPA in complex with fibronectin domains. *Proc Natl Acad Sci USA* **105:** 12254–12258.

Bisno, A.L., Rubin, F.A., Cleary, P.P., and Dale, J.B. (2005) Prospects for a group A streptococcal vaccine: rationale, feasibility, and obstacles – report of a National Institute of Allergy and Infectious Diseases Workshop. *Clin Infect Dis* **41:** 1150–1156.

Brown, L.F., Dubin, D., Lavigne, L., Logan, B., Dvorak, H.F., and Van De Water, L. (1993) Macrophages and fibroblasts express embryonic fibronectins during cutaneous wound healing. *Am J Pathol* **142:** 793–801.

Carapetis, J., Steer, A., Mulholland, E., and Weber, M. (2005) The global burden of group A streptococcal diseases. *Lancet Infect Dis* **5:** 685–694.

Caswell, C., Lukomska, E., Seo, N., Höök, M., and Lukomski, S. (2007) Scl1-dependent internalization of group A *Streptococcus* via direct interactions with the $\alpha_2\beta_1$ integrin enhances pathogen survival and re-emergence. *Mol Microbiol* **64:** 1319–1331.

Caswell, C.C., Barczyk, M., Keene, D.R., Lukomska, E., Gullberg, D.E., and Lukomski, S. (2008a) Identification of the first prokaryotic collagen sequence motif that mediates binding to human collagen receptors, integrins $\alpha_2\beta_1$ and $\alpha_{11}\beta_1$. *J Biol Chem* **283:** 36168–36175.

Caswell, C.C., Han, R., Hovis, K.M., Ciborowski, P., Keene, D.R., Marconi, R.T., *et al.* (2008b) The Scl1 protein of M6-type group A *Streptococcus* binds the human complement regulatory protein, factor H, and inhibits the alternative pathway of complement. *Mol Microbiol* **67:** 584–596.

Caswell, C.C., Oliver-Kozup, H., Han, R., Lukomska, E., and Lukomski, S. (2010) Scl1, the multifunctional adhesin of group A *Streptococcus*, selectively binds cellular fibronectin and laminin, and mediates pathogen internalization by human cells. *FEMS Microbiol Lett* **303:** 61–68.

Chhatwal, G.S., and Preissner, K.T. (2000) Extracellular matrix interactions with gram-positive pathogens. In *Gram-Positive Pathogens*. Fischetti, V.A., Novick, R.P., Ferretti, J., Portnoy, D.A., and Rood, J.I. (eds). Washington, D.C.: ASM Press, pp. 78–86.

Cho, K., and Caparon, M. (2005) Patterns of virulence gene expression differ between biofilm and tissue communities of *Streptococcus pyogenes*. *Mol Microbiol* **57:** 1545–1556.

Connolly, K.L., Roberts, A.L., Holder, R.C., and Reid, S.D. (2011) Dispersal of Group A streptococcal biofilms by the cysteine protease SpeB leads to increased disease severity in a murine model. *PLoS ONE* **6:** e18984.

Courtney, H.S., Chiang, H.C., Thacker, J.L., and Dale, J.B. (1999) Serum opacity factor is a major fibronectin-binding protein and a virulence determinant of M type 2 *Streptococcus pyogenes*. *Mol Microbiol* **32:** 89–98.

Courtney, H.S., Hasty, D.L., and Dale, J.B. (2003) Serum opacity factor (SOF) of *Streptococcus pyogenes* evokes antibodies that opsonize homologous and heterologous SOF-positive serotypes of group A streptococci. *Infect Immun* **71:** 5097–5103.

Courtney, H.S., Li, Y., Twal, W.O., and Argraves, W.S. (2009)

Serum opacity factor is a streptococcal receptor for the extracellular matrix protein fibulin-1. *J Biol Chem* **284:** 12966–12971.

Cramer, T., Yamanishi, Y., Clausen, B.E., Forster, I., Pawlinski, R., Mackman, N., *et al.* (2003) HIF-1α is essential for myeloid cell-mediated inflammation. *Cell* **112:** 645–657.

Cue, D., Lam, H., and Cleary, P.P. (2001) Genetic dissection of the *Streptococcus pyogenes* M1 protein: regions involved in fibronectin binding and intracellular invasion. *Microb Pathog* **31:** 231–242.

Dillon, H.C., and Wannamaker, L.W. (1971) Skin infections and acute glomerulonephritis, report of a symposium. *Mil Med* **136:** 122–127.

Dillon, H.C., Derrick, C.W., and Dillon, M.S. (1974) M-Antigens common to pyoderma and acute glomerulonephritis. *J Infect Dis* **130:** 257–267.

Ensenberger, M.G., Tomasini-Johansson, B.R., Sottile, J., Ozeri, V., Hanski, E., and Mosher, D.F. (2001) Specific interactions between F1 adhesin of *Streptococcus pyogenes* and N-terminal modules of fibronectin. *J Biol Chem* **276:** 35606–35613.

Ffrench-Constant, C., Van De Water, L., Dvorak, H.F., and Hynes, R.O. (1989) Reappearance of an embryonic pattern of fibronectin splicing during wound healing in the adult rat. *J Cell Biol* **109:** 903–914.

Gao, Y., Liang, C., Zhao, R., Lukomski, S., and Han, R. (2010) The Scl1 of M41-type group A *Streptococcus* binds the high-density lipoprotein. *FEMS Microbiol Lett* **309:** 55–61.

Green, N., Zhang, S., Porcella, S., Nagiec, M., Barbian, K., Beres, S., *et al.* (2005a) Genome sequence of a serotype M28 strain of group A *Streptococcus*: potential new insights into puerperal sepsis and bacterial disease specificity. *J Infect Dis* **192:** 760–770.

Green, N.M., Beres, S.B., Graviss, E.A., Allison, J.E., McGeer, A.J., Vuopio-Varkila, J., *et al.* (2005b) Genetic diversity among type *emm28* group A *Streptococcus* strains causing invasive infections and pharyngitis. *J Clin Microbiol* **43:** 4083–4091.

Han, R., Caswell, C.C., Lukomska, E., Keene, D.R., Pawlowski, M., Bujnicki, J.M., *et al.* (2006a) Binding of the low-density lipoprotein by streptococcal collagen-like protein Scl1 of *Streptococcus pyogenes*. *Mol Microbiol* **61:** 351–367.

Han, R., Zwiefka, A., Caswell, C.C., Xu, Y., Keene, D.R., Lukomska, E., *et al.* (2006b) Assessment of prokaryotic collagen-like sequences derived from streptococcal Scl1 and Scl2 proteins as a source of recombinant GXY polymers. *Appl Microbiol Biotechnol* **72:** 109–115.

Hanski, E., and Caparon, M. (1992) Protein F, a fibronectin-binding protein, is an adhesin of the group A *Streptococcus Streptococcus pyogenes*. *Proc Natl Acad Sci USA* **89:** 6172–6176.

Henderson, B., Nair, S., Pallas, J., and Williams, M.A. (2011) Fibronectin: a multidomain host adhesin targeted by bacterial fibronectin-binding proteins. *FEMS Microbiol Rev* **35:** 147–200.

Holbrook, K.A., and Smith, L.T. (2002) Morphology and chemical composition of connective tissue: structure of the skin and tendon. In *Connective Tissue and Its Heritable Disorders*. Royce, P.M., and Steinmann, B. (eds). New York, NY: Wiley-Liss, Inc., pp. 19–39.

House-Pompeo, K., Xu, Y., Joh, D., Speziale, P., and Höök, M. (1996) Conformational changes in the fibronectin binding MSCRAMMs are induced by ligand binding. *J Biol Chem* **271:** 1379–1384.

Humphries, J.D., Byron, A., and Humphries, M.J. (2006) Integrin ligands at a glance. *J Cell Sci* **119:** 3901–3903.

Humtsoe, J.O., Kim, J.K., Xu, Y., Keene, D.R., Höök, M., Lukomski, S., and Wary, K.K. (2005) A streptococcal collagen-like protein interacts with the $\alpha_2\beta_1$ integrin and induces intracellular signaling. *J Biol Chem* **280:** 13848–13857.

Jaffe, J., Natanson-Yaron, S., Caparon, M.G., and Hanski, E. (1996) Protein F2, a novel fibronectin-binding protein from *Streptococcus pyogenes*, possesses two domains. *Mol Microbiol* **21:** 373–384.

Jagnow, J., and Clegg, S. (2003) *Klebsiella pneumoniae* MrkD-mediated biofilm formation on extracellular matrix- and collagen-coated surfaces. *Microbiology* **149:** 2397–2405.

Katerov, V., Lindgren, P.E., Totolian, A.A., and Schalen, C. (2000) Streptococcal opacity factor: a family of bifunctional proteins with lipoproteinase and fibronectin-binding activities. *Curr Microbiol* **40:** 149–156.

Kim, J.H., Singvall, J., Schwarz-Linek, U., Johnson, B.J., Potts, J.R., and Höök, M. (2004) BBK32, a fibronectin binding MSCRAMM from *Borrelia burgdorferi*, contains a disordered region that undergoes a conformational change on ligand binding. *J Biol Chem* **279:** 41706–41714.

Kimura, K.R., Nakata, M., Sumitomo, T., Kreikemeyer, B., Podbielski, A., Terao, Y., *et al.* (2012) Involvement of T6 pili in biofilm formation by serotype M6 *Streptococcus pyogenes*. *J Bacteriol* **194:** 804–812.

Kohan, M., Muro, A.F., White, E.S., and Berkman, N. (2010) EDA-containing cellular fibronectin induces fibroblast differentiation through binding to $\alpha_4\beta_7$ integrin receptor and MAPK/Erk 1/2-dependent signaling. *FASEB J* **24:** 4503–4512.

Kreikemeyer, B., Talay, S.R., and Chhatwal, G.S. (1995) Characterization of a novel fibronectin-binding surface protein in group A streptococci. *Mol Microbiol* **17:** 137–145.

Kreikemeyer, B., Klenk, M., and Podbielski, A. (2004) The intracellular status of *Streptococcus pyogenes*: role of extracellular matrix-binding proteins and their regulation. *Int J Med Microbiol* **294:** 177–188.

Lembke, C., Podbielski, A., Hidalgo-Grass, C., Jonas, L., Hanski, E., and Kreikemeyer, B. (2006) Characterization of biofilm formation by clinically relevant serotypes of group A streptococci. *Appl Environ Microbiol* **72:** 2864–2875.

Liao, Y.F., Wieder, K.G., Classen, J.M., and Van De Water, L. (1999) Identification of two amino acids within the EIIIA (ED-A) segment of fibronectin constituting the epitope for two function-blocking monoclonal antibodies. *J Biol Chem* **274:** 17876–17884.

Liao, Y.F., Gotwals, P.J., Koteliansky, V.E., Sheppard, D., and Van De Water, L. (2002) The EIIIA segment of fibronectin is a ligand for integrins $\alpha_9\beta_1$ and $\alpha_4\beta_1$ providing a novel mechanism for regulating cell adhesion by alternative splicing. *J Biol Chem* **277:** 14467–14474.

Lukomski, S., Nakashima, K., Abdi, I., Cipriano, V.J., Ireland, R.M., Reid, S.D., *et al.* (2000a) Identification and characterization of the scl gene encoding a group A *Streptococcus*

extracellular protein virulence factor with similarity to human collagen. *Infect Immun* **68:** 6542–6553.

Lukomski, S., Hoe, N.P., Abdi, I., Rurangirwa, J., Kordari, P., Liu, M., *et al*. (2000b) Nonpolar inactivation of the hypervariable streptococcal inhibitor of complement gene (*sic*) in serotype M1 *Streptococcus pyogenes* significantly decreases mouse mucosal colonization. *Infect Immun* **68:** 535–542.

Lukomski, S., Nakashima, K., Abdi, I., Cipriano, V.J., Shelvin, B.J., Graviss, E.A., *et al*. (2001) Identification and characterization of a second extracellular collagen-like protein made by group A *Streptococcus*: control of production at the level of translation. *Infect Immun* **69:** 1729–1738.

Maddocks, S.E., Wright, C.J., Nobbs, A.H., Brittan, J.L., Franklin, L., Stromberg, N., *et al*. (2011) *Streptococcus pyogenes* antigen I/II-family polypeptide AspA shows differential ligand-binding properties and mediates biofilm formation. *Mol Microbiol* **81:** 1034–1049.

Manetti, A., Zingaretti, C., Falugi, F., Capo, S., Bombaci, M., Bagnoli, F., *et al*. (2007) *Streptococcus pyogenes* pili promote pharyngeal cell adhesion and biofilm formation. *Mol Microbiol* **64:** 968–983.

Mao, Y., and Schwarzbauer, J.E. (2005) Fibronectin fibrillogenesis, a cell-mediated matrix assembly process. *Matrix Biol* **24:** 389–399.

Margarit, I., Bonacci, S., Pietrocola, G., Rindi, S., Ghezzo, C., Bombaci, M., *et al*. (2009) Capturing host-pathogen interactions by protein microarrays: identification of novel streptococcal proteins binding to human fibronectin, fibrinogen, and C4BP. *FASEB J* **23:** 3100–3112.

Marjenberg, Z.R., Ellis, I.R., Hagan, R.M., Prabhakaran, S., Höök, M., Talay, S.R., *et al*. (2011) Cooperative binding and activation of fibronectin by a bacterial surface protein. *J Biol Chem* **286:** 1884–1894.

Martin, P. (1997) Wound healing-aiming for perfect skin regeneration. *Science* **276:** 75–81.

Mohs, A., Silva, T., Yoshida, T., Amin, R., Lukomski, S., Inouye, M., *et al*. (2007) mechanism of stabilization of a bacterial collagen triple helix in the absence of hydroxyproline. *J Biol Chem* **282:** 29757–29765.

O'Loughlin, R., Roberson, A., Cieslak, P., Lynfield, R., Gershman, K., Craig, A., *et al*. (2007) The epidemiology of invasive group A streptococcal infection and potential vaccine implications: United States, 2000–2004. *Clin Infect Dis* **45:** 853–862.

Oehmcke, S., Podbielski, A., and Kreikemeyer, B. (2004) Function of the fibronectin-binding serum opacity factor of *Streptococcus pyogenes* in adherence to epithelial cells. *Infect Immun* **72:** 4302–4308.

Oliver-Kozup, H.A., Elliott, M., Bachert, B.A., Martin, K.H., Reid, S.D., Schwegler-Berry, D.E., *et al*. (2011) The streptococcal collagen-like protein-1 (Scl1) is a significant determinant for biofilm formation by group A *Streptococcus*. *BMC Microbiol* **11:** 262.

Ozeri, V., Rosenshine, I., Mosher, D.F., Fassler, R., and Hanski, E. (1998) Roles of integrins and fibronectin in the entry of *Streptococcus pyogenes* into cells via protein F1. *Mol Microbiol* **30:** 625–637.

Påhlman, L.I., Marx, P.F., Mörgelin, M., Lukomski, S., Meijers, J.C.M., and Herwald, H. (2007) Thrombin-activatable fibrinolysis inhibitor binds to *Streptococcus pyogenes* by interacting with collagen-like proteins A and B. *J Biol Chem* **282:** 24873–24881.

Palmer, E.L., Ruegg, C., Ferrando, R., Pytela, R., and Sheppard, D. (1993) Sequence and tissue distribution of the integrin α_9 subunit, a novel partner of β_1 that is widely distributed in epithelia and muscle. *J Cell Biol* **123:** 1289–1297.

Pankov, R., and Yamada, K.M. (2002) Fibronectin at a glance. *J Cell Sci* **115:** 3861–3863.

Patti, J.M., Allen, B.L., Mcgavin, M.J., and Höök, M. (1994) MSCRAMM-mediated adherence of microorganisms to host tissues. *Annu Rev Microbiol* **48:** 585–617.

Rasmussen, M., and Björck, L. (2001) Unique regulation of SclB-a novel collagen-like surface protein of *Streptococcus pyogenes*. *Infect Immun* **40:** 1427–1438.

Rasmussen, M., Eden, A., and Björck, L. (2000) SclA, a novel collagen-like surface protein of *Streptococcus pyogenes*. *Infect Immun* **68:** 6370–6377.

Reuter, M., Caswell, C.C., Lukomski, S., and Zipfel, P.F. (2010) Binding of the human complement regulators CFHR1 and factor H by streptococcal collagen-like protein 1 (Scl1) via their conserved C termini allows control of the complement cascade at multiple levels. *J Biol Chem* **285:** 38473–38485.

Roberts, A.L., Connolly, K.L., Doern, C.D., Holder, R.C., and Reid, S.D. (2010) Loss of the group A *Streptococcus* regulator Srv decreases biofilm formation *in vivo* in an otitis media model of infection. *Infect Immun* **78:** 4800–4808.

Rocha, C.L., and Fischetti, V.A. (1999) Identification and characterization of a novel fibronectin-binding protein on the surface of group A streptococci. *Infect Immun* **67:** 2720–2728.

Sakai, T., Johnson, K.J., Murozono, M., Sakai, K., Magnuson, M.A., Wieloch, T., *et al*. (2001) Plasma fibronectin supports neuronal survival and reduces brain injury following transient focal cerebral ischemia but is not essential for skin-wound healing and hemostasis. *Nat Med* **7:** 324–330.

Schierle, C.F., De La Garza, M., Mustoe, T.A., and Galiano, R.D. (2009) Staphylococcal biofilms impair wound healing by delaying reepithelialization in a murine cutaneous wound model. *Wound Repair Regen* **17:** 354–359.

Schmidt, K.H., Mann, K., Cooney, J., and Köhler, W. (1993) Multiple binding of type 3 streptococcal M protein to human fibrinogen, albumin and fibronectin. *FEMS Immunol Med Microbiol* **7:** 135–143.

Serini, G., Bochaton-Piallat, M.L., Ropraz, P., Geinoz, A., Borsi, L., Zardi, L., *et al*. (1998) The fibronectin domain ED-A is crucial for myofibroblastic phenotype induction by transforming growth factor-β_1. *J Cell Biol* **142:** 873–881.

Shinde, A.V., Bystroff, C., Wang, C., Vogelezang, M.G., Vincent, P.A., Hynes, R.O., *et al*. (2008) Identification of the peptid $\alpha_9\beta1$-dependent cellular activities. *J Biol Chem* **283:** 2858–2870.

Singh, P., Reimer, C.L., Peters, J.H., Stepp, M.A., Hynes, R.O., and Van De Water, L. (2004) The spatial and temporal expression patterns of integrin $\alpha_9\beta_1$ and one of its ligands, the EIIIA segment of fibronectin, in cutaneous wound healing. *J Invest Dermatol* **123:** 1176–1181.

Singh, P., Chen, C., Pal-Ghosh, S., Stepp, M.A., Sheppard, D., and Van De Water, L. (2009) Loss of integrin $\alpha_9\beta_1$ results in

defects in proliferation, causing poor re-epithelialization during cutaneous wound healing. *J Invest Dermatol* **129:** 217–228.

Sumby, P., Porcella, S., Madrigal, A., Barbian, K., Virtaneva, K., Ricklefs, S., *et al*. (2005) Evolutionary origin and emergence of a highly successful clone of serotype M1 group A *Streptococcus* involved multiple horizontal gene transfer events. *J Infect Dis* **192:** 771–782.

Talay, S.R., Valentin-Weigand, P., Timmis, K.N., and Chhatwal, G.S. (1994) Domain structure and conserved epitopes of Sfb protein, the fibronectin-binding adhesin of *Streptococcus pyogenes*. *Mol Microbiol* **13:** 531–539.

Taooka, Y., Chen, J., Yednock, T., and Sheppard, D. (1999) The integrin $\alpha_9\beta_1$ mediates adhesion to activated endothelial cells and transendothelial neutrophil migration through interaction with vascular cell adhesion molecule-1. *J Cell Biol* **145:** 413–420.

Tart, A., Walker, M., and Musser, J. (2007) New understanding of the group A *Streptococcus* pathogenesis cycle. *Trends Microbiol* **15:** 318–325.

Terao, Y., Kawabata, S., Kunitomo, E., Murakami, J., Nakagawa, I., and Hamada, S. (2001) Fba, a novel fibronectin-binding protein from *Streptococcus pyogenes*, promotes bacterial entry into epithelial cells, and the *fba* gene is positively transcribed under the Mga regulator. *Mol Microbiol* **42:** 75–86.

Terao, Y., Kawabata, S., Nakata, M., Nakagawa, I., and Hamada, S. (2002) Molecular characterization of a novel fibronectin-binding protein of *Streptococcus pyogenes* strains isolated from toxic shock-like syndrome patients. *J Biol Chem* **277:** 47428–47435.

To, W.S., and Midwood, K.S. (2011) Plasma and cellular fibronectin: distinct and independent functions during tissue repair. *Fibrogenesis Tissue Repair* **4:** 21.

Tognetti, L., Martinelli, C., Berti, S., Hercogova, J., Lotti, T., Leoncini, F., *et al*. (2012) Bacterial skin and soft tissue infections: review of the epidemiology, microbiology, aetiopathogenesis and treatment: a collaboration between dermatologists and infectivologists. *J Eur Acad Dermatol Venereol* **8:** 931–941.

Whatmore, A.M. (2001) *Streptococcus pyogenes sclB* encodes a putative hypervariable surface protein with a collagen-like repetitive structure. *Microbiology* **147:** 419–429.

Xu, Y., Keene, D.R., Bujnicki, J.M., Höök, M., and Lukomski, S. (2002) Streptococcal Scl1 and Scl2 proteins form collagen-like triple helices. *J Biol Chem* **277:** 27312–27318.

Supporting information

Additional supporting information may be found in the online version of this article.